Note on Selfcalibration of EVLA Snapshot Imaging

W. D. Cotton (NRAO) December 22, 2016

***Abstract*—Snapshot imaging with an interferometer array such as the EVLA is prone to having artifacts corresponding to the sidelobes due to the arms of the array. Self calibration is generally used to reduce these but its effectiveness can be limited. Examples are given using EVLA data demonstrating this point.**

***Index Terms*—Radio Interferometry, image artifacts, self calibration**

I. Introduction

INTERFEROMETER arrays such as the EVLA with prominent linear features in the layout of the antennas will have prominent sidelobes in the derived dirty images reflecting the Fourier transform of the linear feature. For an extended synthesis the rotation in parallactic angle will smear out these sidelobes but for single snapshot images they can be prominent. Calibration errors, especially those in phase, will cause artifacts primarily along these linear sidelobes even after deconvolution. Self calibration is an iterative technique to estimate and remove these calibration errors. However, some of the image errors due to the calibration errors will be incorporated into the sky model used for self calibration and will not be removed. This effect can be aggravated by the coarse image grid frequently used. Some of these effects are hard to avoid in automated imaging schemes but can be greatly reduced by an experienced user who can apply additional information to the process. An example of this is shown. The example shown here uses the Obit package ([1], http://www.cv.nrao.edu/∼bcotton/Obit.html).

II. Example Self–calibration

In the following, observations of a strong, inverted spectrum point source (i.e. very unresolved) at S band (2-4 GHz) with the EVLA in B configuration are used. The source in question was approximately 7° from the phase reference calibrator whose observations were approximately 7 min. before and after the target source. 30 seconds were obtained on source. Data were calibrated using the standard Obit calibration pipeline and the imaging used Obit wideband imager MFImage.

Imaging using a standard script with a cell spacing 1/5 of the CLEAN restoring beam (3”) is shown in Figure 1 **Top left**. Imaging used autoboxing to select the CLEAN window, one phase only self calibration and one amplitude and phase self calibration. Strong negative artifacts appear along the images of the EVLA arms. The peak in the image is 605 mJy/bm and the dynamic range 3060.

Repeating the automated imaging using a finer grid (0.35”) yielded the results shown in Figure 1 **Top right**. The artifacts persist but at a much lower level and several fainter sources not visible in the previous version are now visible. The peak in the image is 563 mJy/bm and the dynamic range 5000.

In the imaging procedure, the cause of these artifacts were quite apparent, phase errors in the initial, external calibration left artifacts near the primary response which were then incorporated into the self calibration model resulting in a degraded calibration. Multiple iterations of self-calibration made no substantial improvement.

The inverted spectrum of this AGN indicates that it is very small; small enough to be self–absorbed and completely dominates the emission in the field. Using this information, a “by hand” imaging was done which started from a point source model centered on the position of the peak in the dirty image. This was followed by several iterations of phase only self calibration with CLEAN boxes manually specified. This was followed by an amplitude and phase self calibration; the resultant image is shown in Figure 1 **Bottom**. The image artifacts are almost completely removed. The peak in the image is 644 mJy/bm and the dynamic range 8800. The RMS phase correction from the phase self–cal at the center of the band was 11° which while not terribly good neither is it terribly bad.

III. Discussion

The example shown in Section II shows imaging artifacts produced by an automated imaging script that could be largely be eliminated by a manual processing using additional information not available to the script. Using a cell spacing of 1/8 of the CLEAN restoring beam gave signifigantly better results than a cell spacing of 1/5 of the beam but was still signifigantly degraded with respect to the manual processing. The manual processing used here cannot be applied on a large scale in an automated process but may be necessary if the best image is needed for the science. The example given here is an extreme case (i.e. very simple and bright) as relatively straightforward manual operations resulted in a very improved image. There is likely to be a subset of cases where manual intervention is needed. In the data set from which this example was taken, this was the most extreme of approximately a half dozen of the 200 targets imaged showing this type of artifact.

References

[1] W. D. Cotton, “Obit: A Development Environment for Astronomical Algorithms,” *PASP*, vol. 120, pp. 439–448, 2008.

W. Cotton is with National Radio Astronomy Observatory, 520 Edgemont Rd., Charlottesville, VA, 22903 USA email: bcotton@nrao.edu

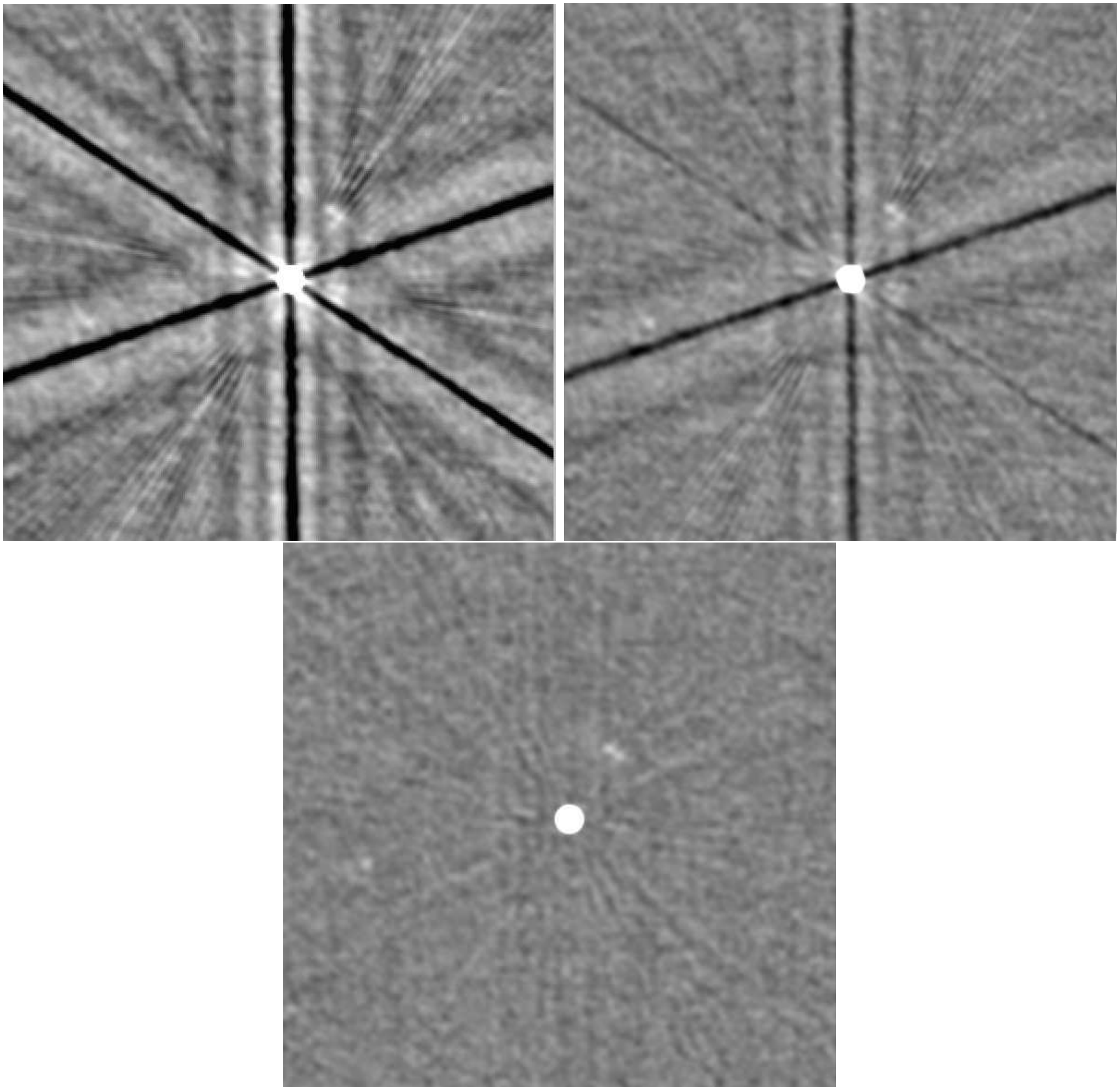

Fig. 1. Results of three imagings of the same data shown using the same transfer function.
Top left: Automated imaging with autoboxing and one phase self calibration followed by amplitude and phase self-cal. Cell spacing = 0.6”.
Top right: Like **Top left:** but using 0.35” cell spacing.
Bottom: Initial point source calibration followed by hand imaging with 2 phase self calibrations and one amplitude and phase self calibration. Cell spacing = 0.37”.